©ISTOCKPHOTO.COM/DEMAERRE

Exploring 3-D Printing for New Applications

*Ryan Bahr,
Bijan Tehrani, and
Manos M. Tentzeris*

This article outlines a number of inkjet-/three-dimensional (3-D)-printed prototypes of RF and millimeter-wave (mmW) components, interconnects, and systems. We pay special attention to the major challenges related to applying current multidimensional printing technologies to the fabrication of flexible multichip modules (MCMs) and high-performance mmW components.

*Ryan Bahr (rbahr3@gatech.edu), Bijan Tehrani (btehrani3@gatech.edu), and Manos M. Tentzeris (etentze@ece.gatech.edu)
are with the School of Electrical and Computer Engineering, Georgia Institute of Technology, Atlanta, United States.*

The explosive growth of state-of-the-art wireless and RF technologies for communication, sensing, and energy harvesting applications requires low-loss interconnects as well as ever-increasing bandwidth and shrinking package sizes.

Background

The explosive growth of state-of-the-art wireless and RF technologies for communication, sensing, and energy harvesting applications requires low-loss interconnects as well as ever-increasing bandwidth and shrinking package sizes. Additive manufacturing techniques offer an opportunity to tackle these challenges by enabling novel designs that reduce waste, while featuring considerable cost savings in high-volume production. In addition, next-generation specifications (such as IEEE 802.11ad WiGig), along with an increasing number of wearable, conformal, and implantable systems, will further increase the demand for sufficiently capable, flexible, and scalable manufacturing methods to meet their requirements

Additive manufacturing technologies, such as inkjet and 3-D printing, can easily achieve resolutions in the micron range, both for the XY (horizontal-plane) feature size and Z (vertical-layer) height, with inkjet printing excelling at thin-film deposition from tens of nanometers to micrometers. The resulting reduction in the required raw materials and tooling—due to the inherent advantage of depositing material only where necessary—dramatically reduces design expenses. As no additional tooling is required to realize free-space and/or controlled dielectric-varied volumes within the material, it is possible to realize internal voids not feasible using conventional tooling for commonly used subtractive methods. Another advantage shared by many additive manufacturing technologies—in addition to the inherent capability of fabricating multiple models concurrently—is that, in most cases, they involve rapid prototyping with quick turnaround times and reduced design validation costs.

Recent research has demonstrated the feasibility of using additive manufacturing techniques for mmW frequency 3-D interconnects, packaging, chipless sensor platforms, microfluidics, and passive components. Using a combination of these topologies, an entire system-on-package (SoP) would be feasible with appropriately sized features that could enable mmW multichip packaging structures of arbitrary 3-D shapes.

An Overview of Additive Manufacturing Technologies

Inkjet printing has been repeatedly demonstrated as a viable technique for microwave designs, particularly of thin-film and multimaterial RF structures. Additionally, 3-D printing has been demonstrated for a variety of antenna and waveguide designs; however, among the variety of 3-D-printing technologies, there is still room for development. Quite often, 3-D-printing technologies have focused on creating solid free-form objects but have lacked attention to their integration with conventional manufacturing processes within the electronics industry. Although the following sections focus briefly on inkjet printing, fused deposition modeling (FDM), stereolithography (SLA), and material-jetting technologies, this is not an exhaustive list; for example, we do not discuss technologies such as paper-based 3-D printing and laser sintering/melting.

Inkjet Printing

Inkjet printing excels at employing a minimal amount of materials; this is due to the thin-film nature of the technology, which deposits dielectric and conductive layers just hundreds of nanometers thick (although thick-film dielectric layers up to 150 μm have also been implemented) [1]. The system functions via drop-on-demand (DOD), depositing picoliter amounts of material with piezoelectric actuation. A variety of dielectric materials can be used along with conductive inks—often nanoparticle/microparticle dispersions in a solvent that evaporates after deposition. The largest diameter of the particle in the solvent depends on the inkjet nozzle diameter (typically 10–50 μm); as a rule of thumb, particles should be at least 25% smaller than the nozzle diameter.

A wide variety of materials are available for mmW inkjet-printed modules, including silver nanoparticle inks, dielectric polymers [polymethyl methacrylate (PMMA), SU-8, etc.], graphene, and carbon nanotube solutions [2]. Using a multilayer printing process, nearly any substrate can be manufactured on top of virtually any other substrate using a polymer base layer that serves to reduce surface roughness and adjust surface energy. Designs with more than five metal layers have been reported, with layer heights ranging from 200 nm to 200 μm [3]. While the smallest printing resolution is theoretically around 5 μm for many typical inkjet printers, resolutions of 20 μm on the XY can be reliably achieved, depending on the material.

A significant advantage of many inkjet-printed devices, compared to most rigid manufacturing technologies, is their inherent ability to easily integrate with flexible and wearable applications [4].

Fused Deposition Modeling

FDM is often the first technique that comes to mind when 3-D printing is considered. A thermoplastic polymer is fed in granular or filament form to a heated nozzle exceeding the glass transition temperature (t_g) of the polymer and is then extruded in lines to fill a layer. Layers are bound together through heating

during deposition. Due to the directional paths of the deposition, the strength of an FDM-printed structure is anisotropic, and for many systems the resolution is anisotropic as well.

While most FDM systems feature resolutions of approximately 10–100 μm for individual printed-layer thickness, the XY minimum feature size is limited by the nozzle diameter, with 200–400 μm common for brass/steel nozzle systems (an exception is a system from one manufacturer that achieves 12.5 μm with ceramic tips) [5]. Multiple materials can be deposited simultaneously with additional nozzles on the XYZ gantry, and capabilities for laser sintering, DOD, and syringe deposition may be available as add-ons depending on the system. While this FDM 3-D-printing technique is quite common, it is comparatively the most challenging to use for mmW components due to its typical resolution limitations and difficulty to scale for mass manufacturing.

Stereolithography

SLA is another 3-D-printing technique that involves ultraviolet (UV) exposure of liquid photopolymer resins on a per-layer basis to solidify the resin. Two systems are available for exposure: digital light processing (DLP) and laser. DLP selectively exposes the entire layer to UV light, similar to a digital mask, with the resolution of the printer being a function of the focused distance from the digital micromirror device. Laser exposure traces the layer with a UV laser on a path similar to FDM printing, with the resolution limited to the laser spot size. XY resolutions are typically in the 30-μm range for DLP and the 25–150-μm range for the laser spot size, with layer heights of 10–50 μm being common. High resolution can be realized due to the inherent optical nature of this 3-D-printing approach, with the extreme exhibited by two-photon SLA (reaching resolutions near 100 μm) [6].

There are two main methods of SLA printing: top-down and the more recently common bottom-up. In a top-down approach, the printing platform lowers into a vat of liquid photopolymer, and each layer is exposed from the top. This requires using a vat full of resin with a volume equal to the printer's build height (by surface area) and monitoring the leveling of the resin. A bottom-up approach involves a transparent window on the bottom, while the built structure is plate-lifted from the transparent bottom by the layer height and the material is exposed from underneath, thus requiring just a bit more material than the volume of the design being printed.

These features are very amenable to mmW applications, as is readily demonstrated by numerous previously reported mmW prototypes [7]–[9].

3-D Material Jetting

The two main forms of 3-D jetting technology—material and binder jetting—feature similar deposition

Figure 1. *Several 3-D-printed passive components using material jetting. From top row to bottom: a capacitor, inductor, and resistor of various values [13].*

methods but differ fundamentally. Both technologies deposit materials with inkjet nozzles, offering resolutions often characterized by around 600 dots-per-inch with a resulting feature size of approximately 42 μm. Material jetting selectively deposits photopolymers that cure in situ, with a typical minimum layer height of ~16 μm. Simultaneous multimaterial printing is easily achieved with a wide variety of available photopolymers, although electrically conductive materials have not been demonstrated yet (see Figure 1). Compared to SLA, this approach can reduce the amount of used material but comes at the cost of featuring a resolution much more bound to the physical properties of the liquid photopolymer.

In contrast to material jetting, binder jetting solely deposits adhesives. On the print bed, a layer of fine particles is distributed and compressed to the layer height. This layer, consisting of a single material, is typically made up of particles with a diameter of approximately 20 μm (although there have been reports of particles with diameters down to 1 μm) [10], [11]. The inkjet nozzles dispense the adhesive to bind the particles together. A new layer of particles is deposited and then compressed, and the cycle continues for all particle-based layers, with the adhesive acting as the support material that gets recycled at the end of the print. Selective laser printing and selective laser melting work in a similar manner by laying down particles and using a laser to selectively sinter/melt the particles, either conductive or dielectric, in lieu of adhesives.

The differences between material jetting and inkjet printing are minimal. Material jetting always cures the material in situ, prints thick films exclusively (thickness >1 μm), and often has accompanying software to process and print all the layers without any additional user interaction.

Conductive Material Printing and Compatibility

Often, 3-D printing involves the printing of polymers, with relatively recent advances enabling a
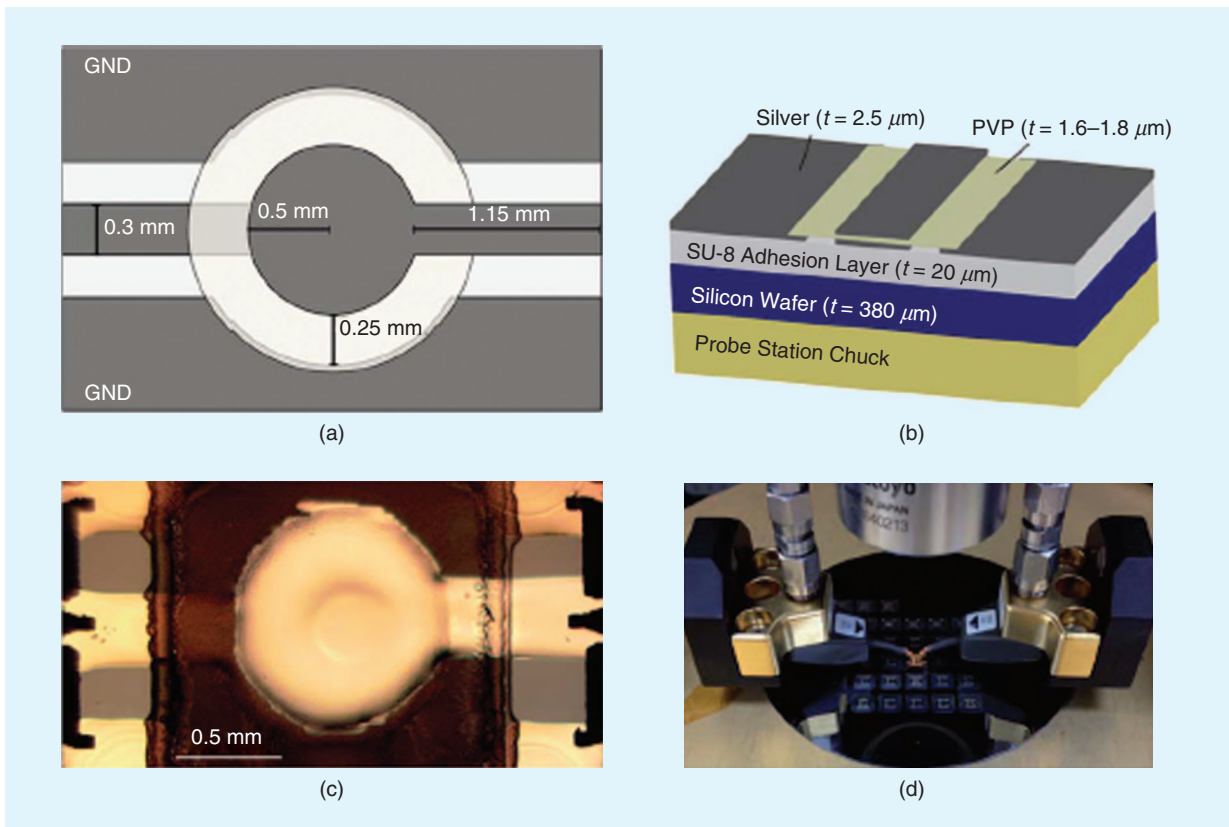
Figure 2. *Modeled and fabricated designs of an inkjet-printed capacitor on silicon substrate: (a) a top-down modeled view, (b) a cross section displaying the topology, (c) an optical micrograph of the capacitor, and (d) the capacitor's probe station measurements [15]. GND: ground; PVP: polyvinylpyrrolidone.*

wide variety of methods to print conductive materials simultaneously or with postprocessing. Of the printing methods discussed in the previous sections, very few deposit the polymer and conductor in an identical manner. For example, inkjet print utilizes the same nozzles for conductive and nonconductive inks, while FDM often requires a syringe deposition system (also known as *direct write*) to deposit highly conductive pastes.

Postprocessing techniques include printing a dielectric design in its entirety and then using a method such as a direct write system, inkjet printing, and aerosol jet printing that deposits conductive materials on the surface of the print. With the appropriate equipment, in most polymer printing methods a dielectric layer can be paused and the conductive layer deposited with the alternative deposition method—although consideration may often be given to any heat treatment used to cure electrically conductive inks and pastes, as well as to the adhesion of the polymer layers that encapsulate any deposited conductors.

The technologies available to deposit conductors are highly dependent on the nature of the design. Aerosol jet printing tends to be one of the more versatile deposition tools, enabling films as thin as 100 nm to be deposited with widths as low as 10 μm, often on

a five-axis deposition system that allows conformal selective coating of complex 3-D designs. Pastes tend to be limited by the syringe deposition system, with 150-μm syringes being common and 12.5 μm [5] using the same systemm as discussed in the "Fused Deposition Modeling" section.

Specific to FDM printing and other thermoplastic dielectrics, copper wiring may be embedded directly, by heating the wire and forcibly injecting it into the print; 3-D-printed microwave designs utilizing this technique have been recently explored [12]. Inkjet printing of conductors for 3-D dielectrics fabrication may require a passivation layer of liquid polymer to reduce the surface roughness of the printed substrate. These materials may also require heat curing to sinter nanoparticles for improved conductivity—although alternative methods exist that expose high irradiance light to the surface of the print, enabling photonic sintering of nanomaterials without subjecting the entire dielectric to high temperatures, which may cause damage or deformation. If applicable to the design, methods that generally completely coat an object, such as electroplating, electroless plating, or sputtering, can be used; these enable controllable layer thickness deposition of ideal electrically conductive elements.

## RF and mmW Printed Passive Components

Passive Devices

Passives are among the most fundamental components necessary for most RF and mmW circuits, with numerous demonstrated printed prototypes using a variety of printing processes and current results showing self-resonant frequencies (SRFs) in the low- to mid-gigahertz ranges. A general rule of thumb is to use discrete components rather than distributed ones when the distances are lower than 0.1 λ; this may make it challenging to fabricate mmW discrete components using many current additive manufacturing technologies.

Inkjet-Printed RF Capacitors

Numerous inkjet- and 3-D-printed metal–insulator–metal (MIM) capacitors have been reported at gigahertz frequencies. Specifically, various inkjet-printed capacitor designs have been demonstrated with SRFs of 1–3 GHz, quality factors of 7.5–25, and capacitances in the range of 10–50 pF, depending on the design; the capacitance per unit area can reach values above 33 pF/mm^2 [14]. These easy-to-scale topologies have also been demonstrated for printing directly onto silicon wafers using a Dimatix DMP-2800 series printer, enabling vertically integrated configurations, as shown in Figure 2 [15].

The ability to print directly onto the silicon substrate enables reduced fabrication costs and minimal parasitics. A detailed look at available printing technologies for RF/mmW modules demonstrates their unique compatibility with many existing technologies due to the relatively low curing temperatures as well as their ability to adhere to different semiconductor substrates.

Typically, silicon presents a difficult printing surface because of its low surface energy, which results in poor wetting [16]. To enable printability on a silicon wafer, three 6.5-μm-thick films of SU-8 are first printed, for a total printed-layer thickness of approximately 20 μm. The SU-8 layer must be baked twice: a pre-exposure bake at 90 °C, followed by a 365-μm UV exposure to crosslink the SU-8 and finished with a postexposure bake of 120 °C. A UV-ozone exposure to increase surface energy for improved wettability is the final step for the fabrication of the isolation/adhesion printed SU-8 layer. The next layer consists of a conductive silver nanoparticle ink (Cabot CCI-300) with five 500-μm layers, for a total thickness of 2.5 μm; this is then baked at 120 °C. Thereafter, depending on the desired RF characteristics, two different dielectric ink formulas are printed with a thickness of 800 nm per layer. The two formulas are made up of a 1-Hexanol solvent containing 1:10 and 1:1 weight per weight percent (w/w%) ratios of poly(4-vinylphenol) and poly(melamine-coformaldehyde); these consist, respectively, of a long-chain polymer and a heat-activated crosslinker. Two layers of each formula are printed, with the 1:10 and
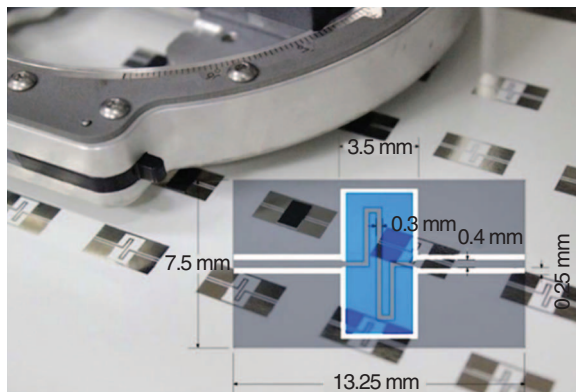
**Figure 3.** An inkjet-printed ferromagnetic nanoparticle meander line inductor [17].

1:1 w/w% reaching 1.6- and 1.8-μm aggregate thicknesses, respectively. A top metallic layer is printed similarly to the first metallic layer, with a postprinting 180 °C bake performed to cure the entire structure.

Inkjet-Printed RF Inductors

Similarly, inductors have been demonstrated on a variety of printing platforms. Novel printed inductors utilizing ferromagnetic nanomaterials (shown in Figure 3) have recently been demonstrated, with the highest quality factor (25+) for printed inductors to date, as shown in an 8-nH inductor with an SRF of 8 GHz [17]. The ferromagnetic nanoparticles have diameters below 200 nm and are coated in a polymer shell (sodium dioctyl sulfosuccinate) to prevent agglomeration and oxidation; these are specifically formulated for the Dimatix DMP 2800 in a way similar to the capacitor printing. The substrate used for the meander inductor is a commercially available photo-paper sheet, upon which five layers of Cabot CCI-300 silver nanoparticle ink were printed, with a 150 °C postprinting bake to sinter the conductive ink. The ferromagnetic ink was then printed for one, three, five, and ten layers. A 150 °C nitrogen oven was used to cure this layer and prevent any additional oxidation.

3-D-Printed RF Capacitors and Inductors

Additionally, 3-D printing has been demonstrated for various MIM capacitor prototypes using material jetting and postprocessing for the metal paste filling, with SRFs up to 1.5 GHz, quality factors of 18–20, and capacitances up to above 14.3 pF [13]. The 3-D-printed passive components were manufactured using a 3-D Systems ProJet HD 3000, with two inks used in creating a dielectric encasing (VisiJet EX 200) and a sacrificial wax (VisiJet S100) to be melted and replaced with silver conductive paste (Pelco 16040-20); the average conductivity was 2.8 x 10^5 S/m. Both materials were deposited in situ through multiple nozzles in the form of 30-μm thick layers. After the printed structure was complete, the entire device was immersed in mineral oil at 80 °C to melt the wax.
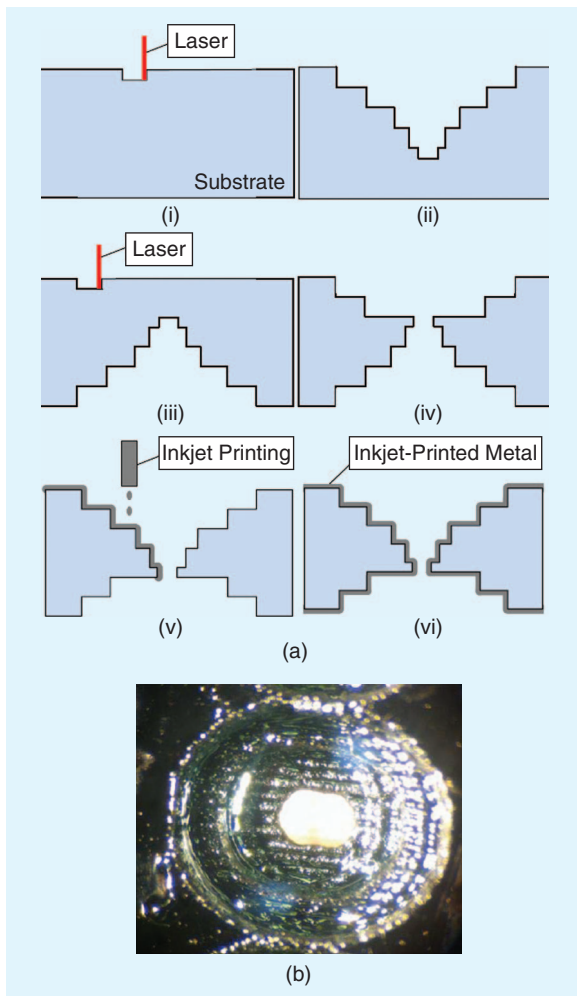
Figure 4. *A multilayer inkjet-printing process for a transformer topology using SU-8 dielectric layers and silver nanoparticle conductive inks [18]. (a) The processes for creating a stepped configuration are demonstrated in (i–vi). (b) The stepped via after inkjet printing. [18].*

Thereafter, a detergent and water bath at 80 °C were used to remove any remaining mineral oil. Last, the liquid metal paste was injected manually into the 600-μm-wide channels to complete the device fabrication. While this topology demonstrates the feasibility of 3-D-printed functional passive components, it also illustrates the fact that automated multilayer conductive printing will be an important next step for many 3-D-printing technologies.

Fully 3-D-printed spiral inductors prototypes have been also realized with the same technique discussed for the capacitors, with a quality factor of 5.6 for 23 nH with an SRF of 1.49 GHz.

Multilayer Inkjet-Printed Transformer

Using processes similar to those described in the "Inkjet-Printed Capacitors" and "Inkjet-Printed Inductors" sections, a fully inkjet-printed multilayer transformer was demonstrated for flexible transformer-based balun designs. As a proof-of-concept demonstrator, a center-tapped 1:2 differential-to-single-ended transformer was designed with a grounded center tap to enable a 180° phase difference between the ports [18]. The primary coil consisted of three turns in parallel, and the secondary coil was a two-turn inductor forming the ratio cited previously.

The six-layer devices, shown in Figure 4, were printed on a 100-μm-thick liquid crystal polymer (LCP) substrate, with feature sizes of 160 μm for the Cabot CCI-300 silver nanoparticle ink traces. The feature resolution/spacing was 200 μm, with the entire inductor having a diameter of 5.6 mm. The thickness of the printed dielectric layer below the bridge was 24 μm, while the maximum available gain of the transformer was –1.7 dB at 1.4 GHz, with the primary and secondary coil inductance measured at 6.1 and 14.2 nH, respectively.

Inkjet-Printed Via

From circuit boards to silicon wafers, vias are a crucial component for most multilayer RF/mmW structures. A via is created by leaving a void in the dielectric substrate and thereafter coating the rim of the void with an electrically conductive material in the form of pastes, plating, or inks.

Various lengths of vias have been additively manufactured, with values ranging from below 100 μm to above 1 mm. In the realm of inkjet-printed vias, the larger vias have been especially challenging to manufacture due to the shrinkage of silver inks during the curing process, with an established process only recently verified. The vias of 1-mm length were fabricated on a PMMA substrate, which was characterized up to 8 GHz using a printed T-resonator [18]. Carbon laser drilling was used to prepare the PMMA substrate for metallization, creating a stair-step structure for the via size of interest, with each step being ~140-μm deep. While the maximum diameter of the via is 1 mm, the volume of the stepped via is similar to that of a conventional cylindrical via, with a uniform diameter of 0.57 mm. An asymmetrical staircase, chosen due to manufacturing constraints involving the laser, effectively improved the transition from the top to the bottom layer of the substrate, as seen in Figure 5, in a topology that is more rugged for flexible implementations.

The via can be modeled as a series resistor and inductor, with the multiple steps characterized as a series of cylinders, the inductance increasing exponentially as the radius decreases, and the resistance varying inversely in proportion to the radius [19]. While the via was used in a demonstration up to 8 GHz, additional considerations for the structure capacitance must be taken into account when the via thickness approaches the wavelength of the design designated for mmW applications. A substrate-integrated-waveguide cavity resonator verifying the performance of the vias was fabricated, with a 5.79-GHz operational frequency and a quality factor of 25.13. The results are low compared to other cavity resonators; this
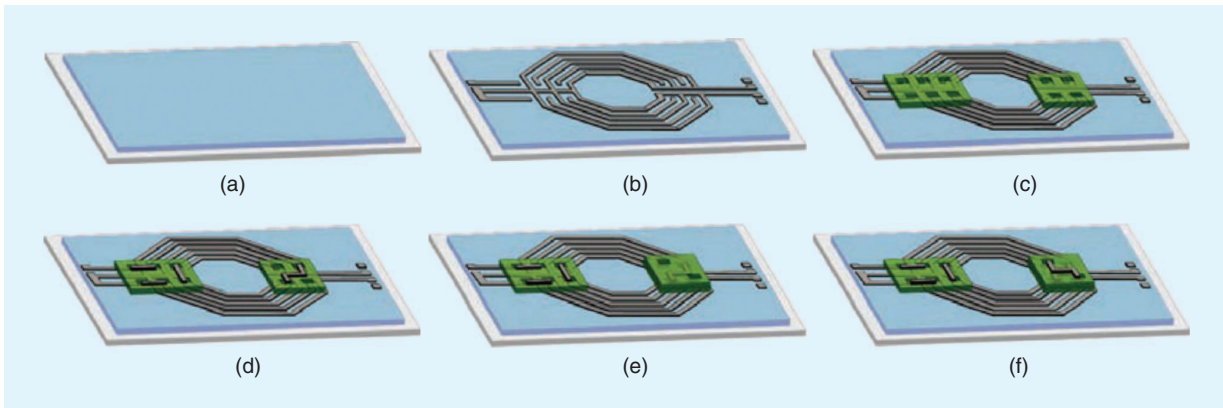
Figure 5. *An asymmetrical stair-stepped via fabrication process using laser drilling and inkjet printing: (a) the adhesion layer, (b) the pattern transformer (M1), (c) the pattern dielectric (D1), (d) the pattern bridges (M2), (e) the pattern dielectric (D2), and (f) the pattern bridge (M3) [19].*

can be attributed to the conductivity being an order of magnitude lower than bulk copper, with the values of 9×10^6 S/m versus 5.96×10^7 S/m for silver nanoparticle ink and bulk copper, respectively.

Other Additively Manufactured Components for mmW Systems

### Stereolithography-Printed Waveguides and Antennas

While no discrete components have been reported using SLA, mmW antennas, metamaterials, dielectric lenses, resonators, filters, and waveguides have been introduced that take advantage of the high process resolution for operation frequencies of 30–300 GHz. Most prototypes have utilized single-dielectric designs and have often used sputtering to metallize the structure. In consideration of a practical mmW MCM, SLA mmW packages containing a combination of these devices could easily be fabricated using this approach.

To realize interchip communications, special metal-coated plastic (MCP) waveguide structures may be beneficial for the low-loss propagation of RF signals up to the sub-terahertz frequency ranges for ultrafast interchip communications. MCP waveguides offer reduced manufacturing times and costs compared to traditional metal-pipe-based waveguides, where the raw material consumption is the most significant component of cost, rather than the machining of the complex designs and topologies.

The Swiss Federal Institute of Technology has demonstrated a 25.4-mm-long WR-3.4-band waveguide, operating at 220–330 GHz, fabricated using SLA techniques and utilizing a layer thickness of 25 μm [20]. The dielectric waveguide was then copper-plated using a custom-developed process, and the fabrication was completed with 100-nm layers of gold on the waveguide flanges. The design operates near the theoretical limit, as seen in Figure 6, while, when terminated with a WR-3.4 smoothed-walled

diagonal horn antenna, it exhibited a 26-dBi maximum directivity throughout the band of operation, with a copolarization content of 90.5%.

A comparison was performed by D'Aruia et al [21] between WR-10 SLA- and WR-90 FDM-printed copper-plated rectangular waveguides. In the SLA printing process, a 3-D Viper si2 containing a laser-based system with a 25-μm spot size was used to print Accura Xtreme resin. The minimum reliable wall thickness was demonstrated to be limited in the region of 140 μm, which was later tested in a filter design. The comparison demonstrated a 4:1 reduction in surface roughness, from 4.99 μm (FDM) to 1.16 μm (SLA) root-mean-square values. The SLA-printed MCP waveguide
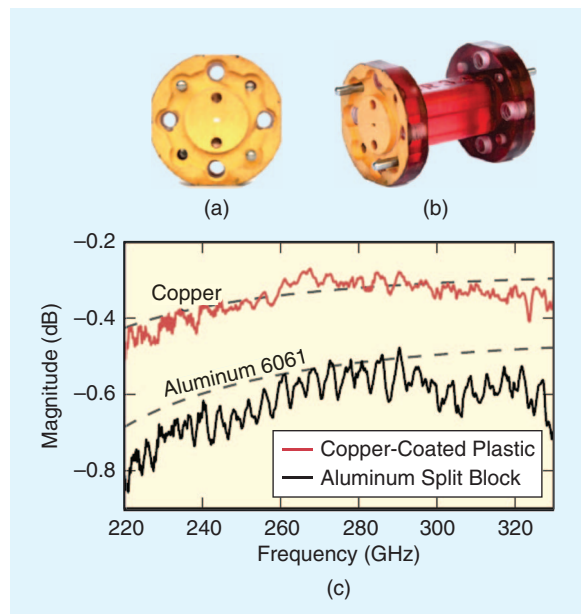
Figure 6. *(a) and (b) The copper SLA-printed MCP waveguide prototype. (c) The S21 of the MCP and aluminum split-block 25.4-mm long waveguides; the dashed lines correspond to the theoretical S21 for each waveguide [20].*

Figure 7. *An inkjet-printed 30-GHz Van-Atta array prototype compared to a traditional credit card-sized RFID tag [22].*
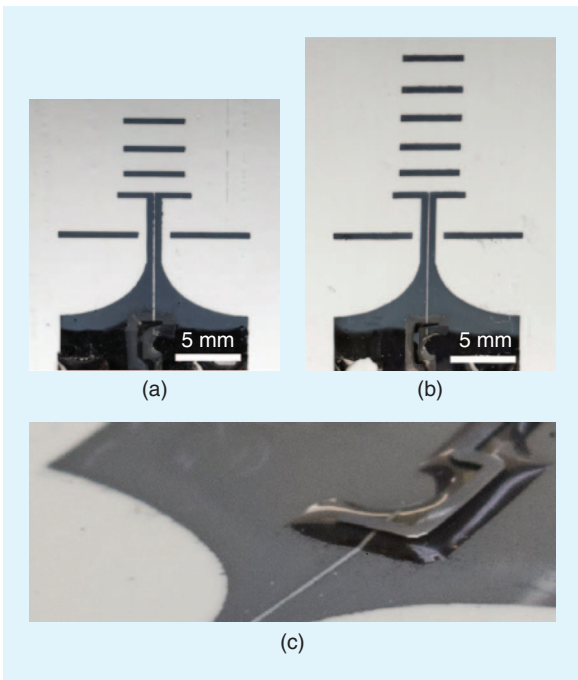
Figure 8. *Inkjet-printed multilayer (a) three-director and (b) five-director Yagi-Uda antenna array prototypes with (c) a detailed image showing the printed dielectric substrate for the microstrip-to-slotline feeding transition [25].*

alleviated unwanted performance issues due to the coupling into an air-filled ring cavity placed between the SLA-printed and the commercial measurement test heads, by adhering a conductive paste to facilitate the connection between flanges. The WR-10 waveguide was demonstrated to feature performance comparable to a similar machined aluminum waveguide, with a dissipative attenuation of 11 dB/m. A sixth-order Chebyshev iris bandpass filter was also fabricated using a split-block design, with 140-μm walls and an electroless plating process for 25-μm copper, demonstrating a 6.8-GHz bandwidth centered at

107.2 GHz and having a loaded and unloaded quality factor of 15.76 and 152, respectively.

Inkjet-Printed mmW Chipless RFID/Humidity Sensor

Taking advantage of the inherent miniaturization of radiative elements, designs that would have previously been too large for specific applications become possible when operating in the mmW range. This is important, especially for state-of-the-art Internet of Things (IoT), smart skins (SS), fifth-generation (5G), autonomous car, and wearable systems, in which size, weight, and power consumption are critical design aspects, while easy scalability to large numbers is fundamental for widespread deployment.

In [22], a fully printed mmW passive system was demonstrated for an inkjet-printed Van-Atta reflect-array topology operating at 30 GHz, consisting of 25 patch antennas on a surface area similar to that of a credit card, as shown in Figure 7. The multifunctional device could simultaneously operate as a range finder, RF identifier (RFID), and humidity sensor by using the Van-Atta reflect-array to maintain a significant radar cross section (RCS) with a scalable aperture size over a wide interrogation angle. The reflected signal was radiated in phase through the antennas toward the direction of the impinging interrogating linear-polarized field with a perpendicular linear polarization to reduce interference. Over a range of 140° (the variation of the angle of incidence of the interrogation signal), the RCS varied by only 10 dB, even for flexed configurations.

To realize a humidity sensor, the series-fed array was inkjet-printed on a polyimide (Kapton) substrate. Using the dielectric constant changes due to different ambient humidity levels resulted in a frequency shift with respect to the interrogation operating frequency that could be easily measured, indirectly determining the sensed humidity values. While small dielectric frequency shifts are traditionally difficult to sense in non-ideal cluttered environments, real-world experiments using this inkjet-printed system have demonstrated an excellent sensing performance for interrogation ranges in excess of 30 m.

Inkjet-Printed mmW High-Gain Antenna Arrays

As we have stressed in previous sections, through a plethora of dielectric polymer and metallic nanoparticle-based inks, inkjet printing offers the advantage of directly fabricating mmW antennas onto virtually any flexible or rigid active-circuit topology and substrate. Specifically, the ability to print thick (> 100-μm) dielectric substrates allows a dramatic reduction in the interconnect length to external antenna structures, realizing miniaturized and highly efficient wireless SoP design solutions, along with reduced material costs that result from additive manufacturing.

In addition to design miniaturization approaches, mmW systems also require the use of high-gain antennas to account for an increased path loss throughout the mmW spectrum and enable such features as selective interrogation and beamsteering for radar, imaging, and high-bandwidth networking applications. Recent efforts have focused on realizing high-gain mmW antennas through inkjet printing fabrication processes, including multilayer proximity-coupled patch-antenna arrays, broadband Vivaldi antennas, and Yagi–Uda array antennas [23]–[25].

Figure 8 shows micrographs of two inkjet-printed 24.5-GHz multidirector Yagi–Uda antenna array prototypes. These antennas were printed onto a low-loss LCP substrate with a metallic silver nanoparticle-based ink. To feed these antennas with a standard microstrip feed, a 3-D microstrip-to-slotline transition was realized through the use of a thick (120-μm) inkjet-printed SU-8 polymer substrate. These printed antennas yielded a positive realized gain over the measured range of 23–26 GHz, with a maximum end-fire realized gain reaching to 6 and 8 dBi for the three- and five-director designs, respectively. The additive fabrication methods used to realize these antennas allow for easy fabrication and integrability of such mmW antennas virtually into/onto the packaging structures, potentially laying the foundation for the first generation of truly flexible, highly integrated mmW systems.

Inkjet-Printed 3-D Interconnects and Antennas for mmW Packaging Topologies

For most practical mmW packages, special attention must be paid to the size of the interconnects, the parasitic effects, the coefficients of thermal expansion, and any detuning that may result from molding or other components in the vicinity of the package. To address these issues, various novel packaging solutions consisting of printed fully 3-D interconnects take advantage of the benefits stemming from high-resolution additive manufacturing. Partially SLA-printed high-speed interconnects have been shown to create new low-crosstalk structures yielding high-density interconnects up to 40 GHz [9].

Additionally, novel fully inkjet-printed 3-D interconnects for silicon dies have been reported using coplanar waveguide (CPW) transmission lines on SU-8 dielectric ramps, as shown in Figure 9. An SU-8 layer was used for die-attachment purposes and realized by inkjet-printing three layers of 4-6 μm (16 μm total), followed by a pre-exposure bake of a 60–120 °C ramp. The 50-μm-thick 2 × 2.7-mm die was manually attached, followed by a UV exposure and postexposure bake of 100 °C. Five additional layers of SU-8 were printed afterward to form the dielectric ramp, and another bake–UV–bake curing process was then performed, finishing with an ozone exposure to tune the surface energy for wetting purposes. The CPW transmission

Recent efforts have focused on realizing high-gain mmW antennas through inkjet printing fabrication processes, including multilayer proximity-coupled patch-antenna arrays, broadband Vivaldi antennas, and Yagi–Uda array antennas.

lines were printed with three layers of Cabot CCI-300 ink before sintering at 180 °C.

The reported prototypes, shown in Figure 10, included inkjet-printed CPW transmission lines on dielectric ramps along with integrated topologies with bow-tie slot antennas. The reported performance results showed minor variations due to the complex morphology of the surface of the fully 3-D-printed structure compared to simulation results, with a 1.5- dB difference across the frequency band of interest for the CPW lines. The 20-μm printing resolution was visible in the design due to the use of tapering gradients for the CPW transition between the different dielectric constants of the die ($\varepsilon_r = 11.4$) and glass packaging substrate ($\varepsilon_r = 4.82$).
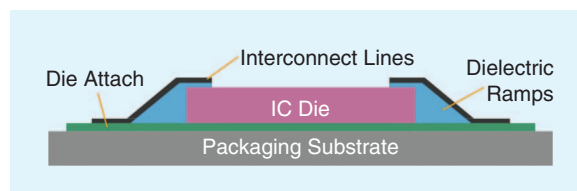
Figure 9. *Inkjet-printed 3-D interconnects (a cross-sectional view) [24].*
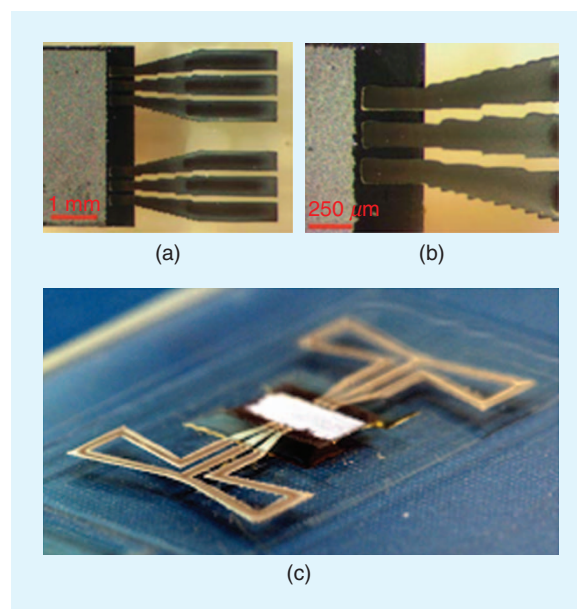
Figure 10. *(a) and (b) Micrographs of on-ramp inkjet-printed CPW lines. (c) A CPW with a slot bow-tie antenna [25].*

This fully printed approach could be easily extended to modules involving multiple silicon dies.

Conclusions

As highlighted in this review, both inkjet and 3-D additive manufacturing techniques have already proven to be disruptive and enabling technologies for fabricating the flexible mmW components and systems that will be essential for the next generation of wireless communication, energy harvesting/transfer, and sensing modules. With the development of all necessary components of a wireless system, including passives, interconnects, and antennas, fully integrated mmW systems can be realized through the selective deposition of metallic and dielectric ink materials, with the additional integration of functionalized nanomaterial inks for high-permeability and environmental-sensing applications.

The inkjet and 3-D-printing techniques discussed here enable the development of highly integrated wireless SoP solutions, enhancing the ease of reconfiguration for quick-turnaround, application-specific product development while challenging traditional MCM packaging technologies with robust 3-D integration. Combining the reconfigurability of additive manufacturing with the benefits of reduced material/tooling costs and production-scale fabrication capabilities, inkjet and 3-D-printing manufacturing techniques are bound to be integral components for the realization of emerging ubiquitous wireless technologies such as the IoT, SS, 5G, and wearable modules.

Acknowledgments

References

[1] L. Yang, A. Rida, R. Vyas, and M. M. Tentzeris, "RFID tag and RF structures on paper substrates using inkjet-printing technology: Part 2," *IEEE Trans. Microwave Theory Tech.*, vol. 55, no. 12, pp. 2894–2901, Dec. 2007.

[2] J. Hester, M. Tentzeris, and Y. Fang, "Inkjet-printed, flexible, high performance, carbon nanomaterial based sensors for ammonia and DMMP gas detection," in *Proc. European Microwave Conf.*, 2015, pp. 857–860.

[3] B. Cook, B. Tehrani, J. Cooper, and M. Tentzeris, "Multilayer inkjet printing of millimeter-wave proximity-fed patch arrays on flexible substrates," *Antennas Wireless Propag. Lett.*, vol. 12, pp. 1351–1354, 2013.

[4] J. Hester, S. Kim, J. Bito, T. Le, J. Kimionis, D. Revier, C. Saintsing, W. Su, B. Tehrani, A. Traille, B. Cook, and M. Tentzeris, "Additively manufactured nanotechnology and origami-enabled flexible microwave electronics," *Proc. IEEE*, vol. 103, no. 4, pp. 583–606, 2015.

[5] (2016). nTip & Accessories. nScrypt. [Online]. Available: http://nscrypt.com/consumables/ntip-accessories

[6] R. Kim and K. Lee, "3-D stereolithography by using two-photon photopolymerization," *Macromolecular Symp.*, vol. 298, no. 1, pp. 25–33, 2010.

[7] P. Timbie, J. Grade, D. van der Weide, B. Maffei, and G. Pisano, "Stereolithographed MM-wave corrugated horn antennas," in *Proc. Int. Conf. Infrared, Millimeter, and Terahertz Waves*, 2011, pp. 1–3.

[8] N. T. Nguyen, N. Delhote, M. Ettorre, D. Baillargeat, L. Le Coq, and R. Sauleau, "Design and characterization of 60-ghz integrated lens antennas fabricated through ceramic stereolithography," *IEEE Trans. Antennas Propagat.*, vol. 58, no. 8, pp. 2757–2762, 2010.

[9] Z. Khan, "A novel transmission line structure for high-speed high-density copper interconnects," *IEEE Trans. Comp. Packag. Manufact. Technol.*, vol. 6, no. 7, pp. 1077–1086, 2016.

[10] N. Arghavan Farzadi, "Effect of layer thickness and printing orientation on mechanical properties and dimensional accuracy of 3-D printed porous samples for bone tissue engineering," *PLoS ONE*, vol. 9, no. 9, p. e108252, 2014.

[11] Y. Bai and C. Williams, "An exploration of binder jetting of copper," *Rapid Prototyping J.*, vol. 21, no. 2, pp. 177–185, 2015.

[12] M. Liang, C. Shemelya, E. MacDonald, R. Wicker, and H. Xin, "3-D printed microwave patch antenna via fused deposition method and ultrasonic wire mesh embedding technique," *IEEE Antennas Wireless Propagat. Lett.*, vol. 14, pp. 1346–1349, 2015.

[13] S. Wu, C. Yang, W. Hsu, and L. Lin, "3-D-printed microelectronics for integrated circuitry and passive wireless sensors," *Microsyst. Nanoeng.*, vol. 1, pp. 15013, June 2015.

[14] B. Cook, J. Cooper, and M. Tentzeris, "Multilayer RF capacitors on flexible substrates utilizing inkjet printed dielectric polymers," *IEEE Microwave Wireless Comp. Lett.*, vol. 23, no. 7, pp. 353–355, 2013.

[15] C. Mariotti, B. Cook, L. Roselli, and M. Tentzeris, "State-of-the-art inkjet-printed metal-insulator-metal (MIM) capacitors on silicon substrate," *IEEE Microwave Wireless Comp. Lett.*, vol. 25, no. 1, pp. 13–15, 2015.

[16] D. Janssen, R. De Palma, S. Verlaak, P. Heremans, and W. Dehaen, "Static solvent contact angle measurements, surface free energy and wettability determination of various self-assembled monolayers on silicon dioxide," *Thin Solid Films*, vol. 515, no. 4, pp. 1433–1438, 2006.

[17] H. Lee, B. Cook, K. Murali, M. Raj, and M. Tentzeris, "Inkjet printed high-Q RF inductors on paper substrate with ferromagnetic nanomaterial," *IEEE Microwave Wireless Comp. Lett.*, vol. 26, no. 6, pp. 419–421, 2016.

[18] B. Cook, C. Mariotti, J. Cooper, D. Revier, B. Tehrani, L. Aluigi, L. Roselli, and M. Tentzeris, "Inkjet-printed, vertically-integrated, high-performance inductors and transformers on flexible LCP substrate," in *Proc. IEEE MTT-S Int. Microwave Symp.*, 2014, pp. 1–4.

[19] S. Kim, A. Shamim, A. Georgiadis, H. Aubert, and M. Tentzeris, "Fabrication of fully inkjet-printed vias and SIW structures on thick polymer substrates," *IEEE Trans. Comp. Packag. Manufact. Technol.*, vol. 6, no. 3, pp. 486–496, 2016.

[20] A. von Bieren, E. de Rijk, J. Ansermet, and A. Macor, "Monolithic metal-coated plastic components for mm-wave applications," in *Proc. 39th Int. Conf. Infrared, Millimeter, and Terahertz Waves*, 2014, pp. 1–2.

[21] M. D'Auria, W. Otter, J. Hazell, B. Gillatt, C. Long-Collins, N. Ridler, and S. Lucyszyn, "3-D printed metal-pipe rectangular waveguides," *IEEE Trans. Comp. Packag. Manufact. Technol.*, vol. 5, no. 9, pp. 1339–1349, 2015.

[22] J. Hester and M. Tentzeris, "Inkjet-printed Van-Atta reflect-array sensors: A new paradigm for long-range chipless low cost ubiquitous smart skin sensors of the internet of things," in *Proc. IEEE MTT-S Int. Microwave Symp.*, May 2016, pp. 1–4.

[23] B. Cook, B. Tehrani, J. Cooper, and M. Tentzeris, "Multilayer inkjet printing of millimeter-wave proximity-fed patch arrays on flexible substrates," *Antennas Wireless Propagat. Lett.*, vol. 12, pp. 1351–1354, 2013.

[24] B. Tehrani, B. Cook, J. Cooper, and M. Tentzeris, "Inkjet printing of a wideband, high gain mm-wave Vivaldi antenna on a flexible organic substrate," in *Proc. IEEE Antennas Propagation Society Int. Symp.*, 2014, pp. 320–321.

[25] B. Tehrani, B. Cook, and M. Tentzeris, "Inkjet printing of multilayer millimeter-wave Yagi–Uda antennas on flexible substrates," *Antennas Wireless Propagat. Lett.*, vol. 15, pp. 143–146, 2016.

[26] B. Tehrani, B. Cook, and M. Tentzeris, "Inkjet-printed 3-D interconnects for millimeter-wave system-on-package solutions," in *Proc. IEEE MTT-S Int. Microwave Symp.*, 2016, pp. 1–4.